

Simulating runaway electrons during disruptions with test particles in the JOREK code

C. Sommariva¹, E. Nardon¹, A. Fil², P. Beyer³, G.T.A. Huysmans¹, M. Hoelzl⁴, D. van Vugt⁵,
K. Sarkimaki⁶ and JET Contributors^{*7}

¹ CEA/DRF/IRFM, 13108, Saint Paul-lez-Durance, France

² PPPL, Princeton University, NJ 08540, Princeton, USA

³ PIIM, Aile 3, Ser. 322, Avenue Escadrille Normandie-Niémen, 13397, Marseille, France

⁴ Max-Planck Institut für Plasmaphysik, 85748, Garching, Germany

⁵ Dep. Applied Physics, T.U. Eindhoven, P.O.B 513, 5600, Eindhoven, Netherlands

⁶ Dep. Applied Physics, P.O.B 14100, FI-00076, Aalto University, Espoo, Finland

⁷ EUROfusion Consortium, JET, Culham Science Center, Abingdon, OX14 3DB, UK

* See the appendix of F. Romanelli et al., *Proceedings of the 25th IAEA Fusion Energy Conference 2014, Saint Petersburg, Russia*

Disruptions are magnetohydrodynamic (MHD) instabilities characterised by a sudden loss of plasma confinement which causes intense heat loads on the plasma facing components, stress on the tokamak structure and the generation of fast particles called runaway electrons. The latter are electrons which are so energetic that the collisional drag is not sufficient to counteract the electric field acceleration. They can reach energies of tens of MeV, representing a serious threat for future tokamak operations [1]. The understanding of runaway electron dynamics and generation mechanisms during a tokamak disruption still represents an open question. The nonlinear MHD code JOREK [2],[3] allows simulating tokamak disruptions induced by massive gas injection (MGI) [4], [5]. Recently, a new JOREK module allowing the tracking of test particles has been implemented. This paper reports on the introduction of the relativistic electron dynamics in the JOREK particle tracker and first applications to study the generation of runaway electrons during a tokamak disruption.

Modelling runaway electrons in the JOREK code

Due to the large difference between the electron gyroperiod ($\tau_e \approx 10^{-11}$ s) and the simulated disruption ($\tau_{dis} \approx 10$ ms) time scales, the full orbit calculation, for a sufficiently large electron population, has a prohibitive computational cost. In order to avoid this problem, the variational relativistic guiding center orbit approximation [6] is used. The guiding center equations of motion are, (please see [6] for symbol definitions):

$$\frac{d\vec{R}}{dt} = \frac{1}{\hat{b} \cdot \vec{B}^*} \left(q\vec{E} \times \hat{b} - p_{\parallel} \frac{\partial \hat{b}}{\partial t} \times \hat{b} + \frac{\mu \hat{b} \times \nabla B}{\gamma} + \frac{p_{\parallel} \vec{B}^*}{m\gamma} \right),$$

$$\frac{dp_{\parallel}}{dt} = \frac{\vec{B}^*}{\hat{b} \cdot \vec{B}^*} \cdot \left(q\vec{E} - p_{\parallel} \frac{\partial \hat{b}}{\partial t} - \frac{\mu \nabla B}{\gamma} \right), \text{ where } \vec{B}^* \equiv p_{\parallel} \nabla \times \hat{b} + q\vec{B}$$

These are resolved using the Cash-Karp 4(5) Runge Kutta method [7] with energy truncation error based time step control. The MHD fields are evaluated from the JOREK solution in both space and time. The space evaluation is performed using 2D Bézier surfaces while the toroidal components are described using Fourier polynomials. The time interpolation is based on a Hermite-Birkhoff scheme so that the field description is globally C^1 . The verification of the guiding center algorithm was performed in a JOREK axisymmetric plasma equilibrium. In this case Noether's theorem states that both total energy and canonical toroidal momentum are invariants of motion so these quantities are used for characterising the code accuracy. Two test cases were considered: a passing particle having an energy of 10 MeV and a pitch angle of 5° and a trapped particle having an energy of 10 keV and a pitch angle of 80° . In both cases,

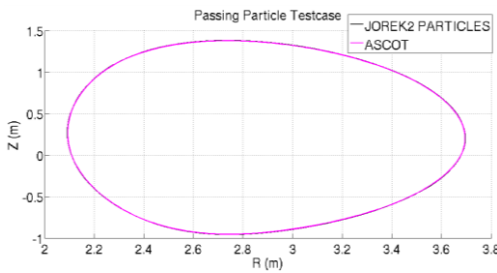


Figure 1: Passing orbit test case

JOREK presented good performances with total energy conservation up to $3 \cdot 10^{-4}$ and $1 \cdot 10^{-5}$, percent of the initial total energy, and canonical toroidal momentum conservation up to $8 \cdot 10^{-3}$ and $1 \cdot 10^{-5}$, percent of the initial toroidal canonical momentum, after a physical time of 2.35 ms. The

same test cases were also used for a benchmark with the ASCOT code [8]. The results are shown in Figure 1 for the passing particle and Figure 2 for the trapped one. As can be seen, the solutions returned by the two codes agree very well. Recently, the Volume Preserving Algorithm [9] for simulating the full orbit trajectory of a particle was implemented. After testing, this routine will be used for verifying the validity of the guiding center approximation in JOREK disruption simulations.

Simulation of runaway electrons in tokamak disruption fields

As a first application, we have computed the evolution of an electron population in the JOREK simulation of an MGI-triggered disruption in the JET 86887 discharge [5]. The magnetic field evolution is visualized via Poincaré plots (Figures 3 to 5).

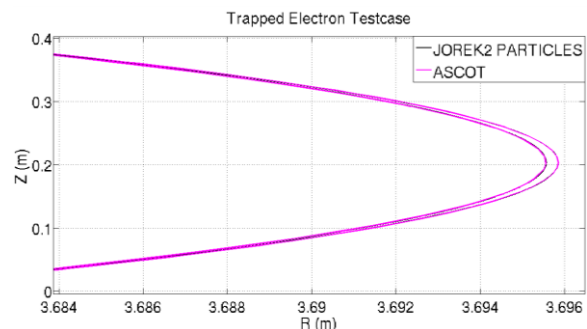


Figure 2: Trapped orbit test case

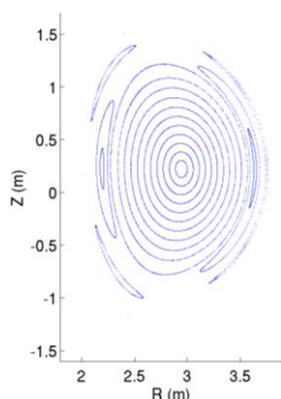


Figure 3: Pre-thermal quench

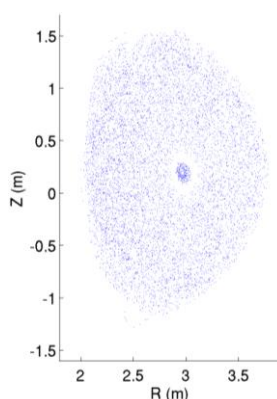


Figure 4: Thermal quench

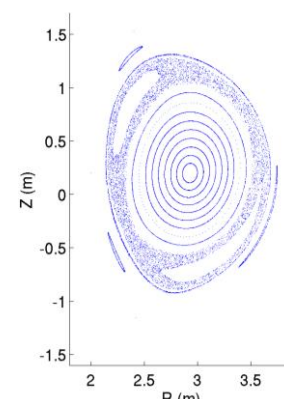


Figure 5: Current quench

Three consecutive phases may be identified: first, the MGI cools down the plasma through dilution and radiation, which destabilizes large MHD modes (Figure 3). These modes excite smaller ones causing the appearance of a large stochastic region which increases its size until the thermal quench (Figure 4).

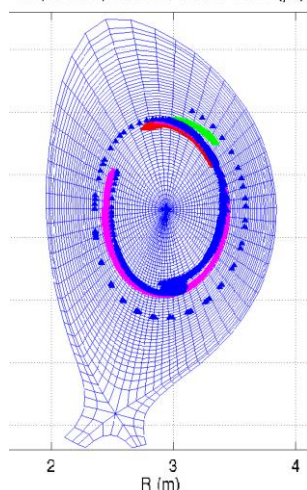
FZ particle positions, time: 0-35.09 (μ s)

Figure 6: RE: Pre-thermal quench

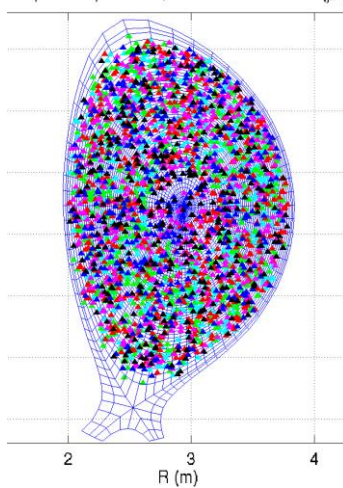
RZ particle positions, time: 153.07-278.25 (μ s)

Figure 7: RE: Thermal quench

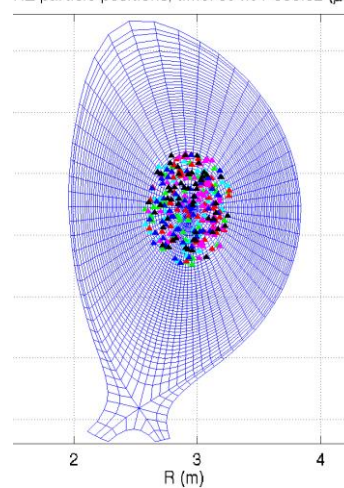
RZ particle positions, time: 694.91-803.32 (μ s)

Figure 8: RE: Current quench

This phase is characterized by a fully developed chaotic region causing the loss of plasma thermal energy confinement. The temperature reduction during the thermal quench implies an increase of resistivity with consequent reduction of plasma current. In the current quench phase (Figure 5) the plasma current rapidly decreases, generating an accelerating electric field. During this phase, well behaved magnetic flux surfaces are reformed progressively, starting from the core of the plasma. A population of 1000 electrons having an energy of 1 keV and a pitch angle of 10° at $3.4 \leq R(m) \leq 3.41$, $0.2162 \leq Z(m) \leq 0.2261$, $\varphi = 0^\circ$ was initialised in the pre-thermal quench phase and followed for all the JOREK simulation. The electrons distribute firstly around the magnetic surfaces (Figure 6) without diffusing in all the plasma bulk until the appearance of magnetic chaos. As soon as the thermal quench takes place (Figure 7), the population starts to diffuse and to be deconfined due to the loss of closed magnetic flux

surfaces but not all the electrons are lost in this phase. In fact, a small fraction of the initial population (6%) is diffused into the plasma core which is the region where the magnetic surfaces reform first after the thermal quench. These forbid the electronic diffusion during the current quench phase (Figure 8). The presence of an electric field causes the acceleration of the surviving population up to tens of MeV (Figure 9). Although

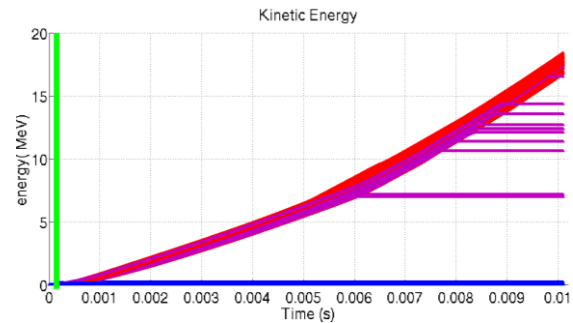


Figure 9: RE: Kinetic energy profile. Blue lines are particles lost at the thermal quench. Magenta lines are particles lost after the thermal quench. Red lines are particles which are never lost. The green line specifies the thermal quench time.

these results are interesting with respect to the possibility of the hot-tail mechanism [10], they should be taken with caution. Indeed, there are reasons to think that the MHD activity is underestimated in these simulations [5]. It has to be remarked that the collisional effects are not included in the presented simulations. However, these should not influence the transport behavior because the Kolmogorov length is smaller than the mean free path so the particle dynamics is dominated by the field stochasticity [11]. On the other hand, the particle final energy might be overestimated due to the absence of collisional drag. A collision operator will be implemented in the near future.

Acknowledgement

This work has been carried out within the framework of the EUROfusion Consortium and has received funding from Euratom research training programme 2014-2018 under the grant agreement No 633053. The views and opinions expressed herein do not necessarily reflect those of the European Commission

References

- [1] M. Lehnen, J. of Nucl. Mat., vol.463, pp.39, 2015
- [2] O. Czarny, G.T.A. Huijsmans, J. Comput. Phys., vol. 227, pp.7423, 2008
- [3] G.T.A. Huijsmans, O. Czarny, Nucl. Fusion, vol.47, pp.659, 2007
- [4] A. Fil et al., Physics of Plasmas, vol. 22, pp. 062509, 2015
- [5] E. Nardon et al., to be submitted to Plasma Phys. and Control. Fusion
- [6] J.R. Cary, A.J. Brizard, Rev. Mod. Phys., vol.81, pp.693, 2009
- [7] J.R. Cash, A.H. Karp, ACM Trans. on Math. Soft., vol.16, pp.201, 1990
- [8] H. Hirvijoki, Comp.Phys.Comm., vol.185, pp.1310, 2014
- [9] R. Zhang et al., P.o.P., vol.22, pp.044501, 2015
- [10] S.C. Chiu et al., Nucl. Fusion., vol.38, pp.1711, 1998
- [11] A.B. Rechester, M.N. Rosenbluth, Phys. Rev. Lett., vol.40, pp.38, 1978